Optimization of GaN Growth Conditions for Improved Device Performance

Joachim Hertkorn

By accurately optimizing the growth conditions for an oxygen doped AlN nucleation layer and for the subsequent epitaxial process the crystal quality of our GaN could drastically be improved. In X-ray diffraction (XRD) analyses we observed FWHM values of 39 arcsec and 114 arcsec for the symmetric (004) and asymmetric (114) reflection, respectively. Consequently, the nominally undoped samples showed semi-insulating behavior in Hall-measurements. By in-situ deposition of a SiN interlayer, the dislocation density could be reduced by more than a factor of 2, reaching a value of $4 \cdot 10^8\ cm^{-2}$*. Samples with this low dislocation density showed an extremely narrow X-ray FWHM of 71 arcsec for the asymmetric (114) reflection along with a narrow linewidth of* $870\,\mu eV$ *in photoluminescence (PL) for the donor bound exciton* (D^0X) *at a temperature of 10 K. Atomic force microscopy (AFM) yielded a very low rms-roughness of about 0.14 nm across a* $4\,\mu m^2$ *scan area. Finally, the excellent crystal quality could be confirmed by growing AlGaN/AlN/GaN heterostructures with a low sheet resistance of* $330\,\Omega/\square$.

1. Introduction

The growth of GaN is still known to be problematic because of the lack of lattice-matched substrates. Therefore a low-temperature nucleation layer consisting of AlN [1] or GaN [2] has to be applied as initial growth step before the deposition of the GaN material. With optimized growth conditions for the nucleation layer (NL) one has to find accurate growth conditions for the GaN-buffer layer which is responsible for the device performance. The grown material has to be optimized in terms of background doping and surface roughness, as well as excellent properties in X-ray diffraction and photoluminescence are desirable. Looking at those parameters one has to remember that the large lattice mismatch (13,8 %) between the GaN epitaxial layer and the applied sapphire substrate results in high dislocation densities up to $2 \cdot 10^9\,\mathrm{cm}^{-2}$ [3]. As this can be seen as a limitation for the performance of many GaN-based devices [4, 5, 6, 7] the in-situ deposition of a SiN interlayer [8, 9, 10, 11] is a simple method to reduce the dislocation density. The treatment of the GaN layer with ammonia (NH_3) and silane (SiH_4) leads to a fractional coverage of the surface with SiN which can act as a nano mask and influence the morphology of the overgrown GaN layer leading to a defect reduction.
In this study we investigate the optimization of the growth conditions for an oxygen doped AlN nucleation layer enabling the stable growth of high quality GaN. Therefore, we studied the influence of oxygen during the nucleation. Afterwards, we focus on the influence of the annealing step right after the nucleation layer deposition as well as the growth

parameters during the GaN-buffer layer deposition and the influence of a SiN interlayer on the dislocation density are under investigation. The increased carrier mobility in the AlGaN/AlN/GaN heterostructures which we finally used as a cross check for our material quality was a result of the defect reduction, as we will describe here.

2. Experimental

The samples were grown by metalorganic vapor phase epitaxy (MOVPE) in an AIXTRON 200/RF-S horizontal flow reactor. All layers were grown on 2" c-plane (0001) epi-ready sapphire wafers slightly miscut by about 0.3 ° towards a-plane using an oxygen doped AlN nucleation [12, 13]. Oxygen doping was done with a mixture of 0.3 % oxygen in nitrogen. Before deposition, the substrates went through in-situ annealing [14] at 1200 °C for 10 min in a hydrogen atmosphere. A reduced reactor pressure between 100 and 200 mbar and the standard precursors trimethyl-aluminum (TMAl), trimethyl-gallium (TMGa), and high purity ammonia were used to deposit the NL and the nominally undoped GaN layer, respectively. The carrier gas was Pd-diffused hydrogen. We fixed the GaN-buffer layer growth parameters in order to establish a high growth rate (1.9 µm/h). Hence we used a TMGa flow of 21 sccm (82 µmol/min) and a V/III-ratio of 1100. The temperature was set to 1140 °C. The GaN was deposited for 1 hour, so we had a buffer layer thickness of around 2 µm. The SiN intermediate layer was integrated after the optimization of the buffer layer growth conditions (sec. 6.).
The crystal quality of our layers was evaluated by high resolution X-ray diffraction (HRXRD) and low temperature (10 K) photoluminescence [15]. The HRXRD measurements were performed without any slits on the detector side. The dislocation density of our layers was determined by atomic force microscopy (AFM) after an HCl etch in our HVPE system [16, 17, 18]. The electrical properties were analyzed by van-der-Pauw Hall measurements at room temperature (295 K) and at liquid nitrogen temperature (77 K). The surface properties on a µm and nm scale were investigated by Nomarski differential interference contrast microscopy (DIC) and AFM, respectively.

3. Oxygen Doped AlN Nucleation

All samples were grown in a four step process (Fig. 1). After thermal cleaning we cooled down to 950 °C and started nucleation. Next was a 360 sec annealing step under hydrogen atmosphere and constant ammonia flow. Here the temperature was set to 1140 °C. Subsequently 2 µm thick GaN layers were deposited under the growth conditions described above. To optimize the AlN nucleation layer, the oxygen content and the ammonia flow, the reactor pressure and the thickness of the layer were varied controlling in particular four figures of merit: The FWHM of the rocking curves of the GaN (002) and (114) peaks, the FWHM of the donor bound exciton measured in PL at 10 K and the surface flatness. In our initial experiment on the AlN nucleation we used a reactor pressure of 100 mbar, a high ammonia flow of 2000 sccm and a TMAl flow of 17 sccm. The massflow of our oxygen source was set to 8 sccm resulting in a calculated O_2-concentration of about 3 ppm. The deposition time was 10 min. As we observed prereactions between NH_3 and TMAl,

Table 2: Summary of the measured FWHM in X-ray and PL after each optimization step.

Optimized Step	X-ray-FWHM (arcsec) (002)-reflex	(114)-reflex	PL-FWHM (μeV) D^0X-Exciton
2	66	137	1590
3	44	117	1650
4	43	116	1190
SiN	82	71	870

we fixed the TMAl flow to 25 sccm (TMAl/O_2 ≈ 5.7) and reduced the ammonia flow to 250 sccm. Finally we could achieve samples with extremely narrow X-ray peaks along with an acceptable surface roughness as observed by DIC (Fig. 2). The PL linewidth was quite promising (Table 2). In order to investigate the influence of the oxygen doping on the nucleation layer, we fixed the optimum parameters as described above and set the oxygen flow to 5 sccm. This yields a calculated O_2-concentration of 2 ppm. Even for such small concentrations, the oxygen influence on the subsequently deposited GaN is significant. In X-ray a linewidth of about 400 arcsec for the (002)-reflection was determined along with a rough surface, resulting in a large rms roughness value of 4.9 nm across a 100 μm^2 scan area. In comparison, the sample with higher oxygen flow showed a relatively smooth surface in AFM with a rms roughness value of 1.7 nm. This experiment demonstrates impressively the need of low oxygen doping during the growth of the AlN nucleation layer. We suppose that the formation of an aluminumoxynitride layer close to the Al_2O_3-substrate is the explanation for our observations. As the reproducibility was improved with a temperature of 920 °C and 10 sccm oxygen flow during the nucleation layer growth, we used these parameters during the following experiments.

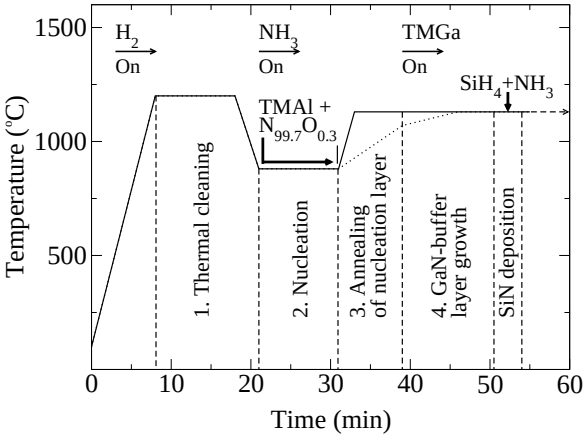

Fig. 1: Temperature ramps during our four step growth process. The temperatures, the ramping-slope and the deposition times were varied in the experiment.

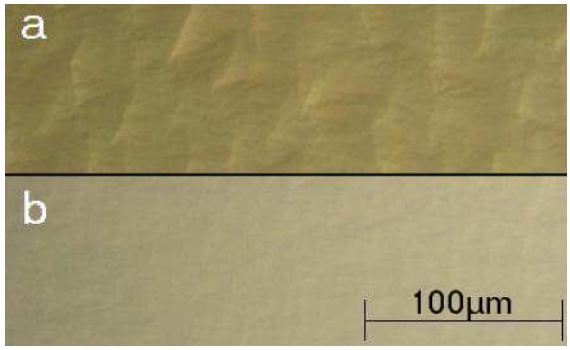

Fig. 2: DIC pictures of two samples with non optimized (a) and optimized (b) annealing step conditions, respectively.

4. Optimization of the Annealing Step After the NL Growth

After optimization of the nucleation layer we studied the influence of annealing as the third process step (Fig. 1) on the GaN quality and surface roughness. Before the optimization of this process step we were used to ramp the reactor temperature to 1140 °C after the deposition of the nucleation layer. Finally the GaN growth was started by opening the TMGa valve after 6 minutes annealing at the chosen temperature (Fig. 1). With these annealing conditions we observed a patterned surface like it is depicted in Fig. 2 (a).
In a first optimization step, we implemented a temperature ramp from 920 °C to 1100 °C in 5 min. There was no additional annealing time with constant temperature. The final GaN growth temperature of 1140 °C was reached during the growth after a second ramp of 7 min. As this improved the crystal quality, we reduced the duration of the first ramp in two steps to 2 min and finally 40 sec. A further reduction was impossible due to the limited heating power of 20 kW. With this extremely short temperature ramp of 40 sec we achieved a smooth surface as illustrated in Fig. 2 (b). The remaining roughness is hardly visible in the interference contrast microscopy. AFM yielded a rms roughness value of 0.9 nm across a 100 μm^2 scan area. The FWHM of the (114)-reflection was hardly affected (Table 2) whereas the FWHM of the (002)-reflection was reduced to the very small value of 44 arcsec. This could mean that under the given conditions the number of threading dislocations is more reduced than that of the edge dislocations [19]. Consequently, edge dislocations might be responsible for the remaining surface roughness in the nanometer range [13, 20]. The influence of the changed annealing conditions on the PL was negligible (Table 2). In agreement with Sugiura et al. we think that mechanisms like recrystallization, decomposition and surface stress relief might be responsible for the discussed effects.

5. Optimization of the GaN Growth Conditions

Finally, we studied the growth conditions during the GaN-buffer layer deposition. As AlGaN/AlN/GaN heterostructures should be used as a probe for our GaN material quality, we decreased the reactor pressure to 100 mbar during the whole growth process as it is normal to prevent prereactions between TMAl and NH_3 during the Al(Ga)N growth. This resulted in an increased GaN growth rate of 2.4 µm/h. The reason might be the increased gas flow speed in the reactor accelerating the material transport.
Due to the changed growth conditions the crystal properties were improved. We observed surface smoothing in the µm and nm ranges, as well as reduced values for the FWHM in the X-ray measurements (Table 2). The rms value determined by AFM across a 100 μm^2 scan area could be reduced to 0.5 nm. The PL linewidth of the D^0X-peak was in the range of 1.2 meV at 10 K. The layer was nominally undoped and showed semi-insulating behavior in van-der-Pauw resistivity measurements. Based on these improvements all samples in the following experiments were grown with a reactor pressure of 100 mbar.

6. Defect Reduction with SiN as Interlayer

Although most properties of the GaN layers could be dramatically improved as discussed above, we still found a relatively high dislocation density ($1 \cdot 10^9\,cm^{-2}$) in those optimized

GaN samples. In order to reduce the dislocation density we ran experiments with a defect-terminating SiN interlayer, which was deposited after the growth of around 500 nm GaN material. For its deposition we decreased the NH_3 flow to 500 sccm, stopped the Ga flow and opened the silane source. Information on the type of dislocation which was reduced most efficiently was obtained by X-ray measurements using the symmetric (002)-reflection and the asymmetric reflections (104) and (114), respectively, as proposed by Heying et al. It is recognized from Fig. 3 that the SiN interlayer was highly effective reducing the dislocation density. The EPD was reduced to $4 \cdot 10^8\,\mathrm{cm}^{-2}$. Based on X-ray measurements we concluded, that mainly edge dislocations were reduced by the SiN interlayer as the asymmetric reflections became extremely narrow. We observed a linewidth of 71 arcsec (114-reflection) and 45 arcsec (104-reflection), respectively. Compared to GaN without a SiN interlayer this was almost a factor of two (Table 2). Thus there is agreement between X-ray measurements and etch pit densities. In addition the reduced edge dislocation density led to a smoothing of the surface in the nanometer range. Finally we measured an extremely low rms roughness value of about 0.14 nm across a $4\,\mu\mathrm{m}^2$ scan area. A slightly increased roughening visible in DIC (not shown) might be traced back to the SiN masking. The excellent crystal quality is confirmed by PL (Fig. 3). The spectrum is dominated by the neutral donor-bound exciton (D^0X) line at 3.486 eV representing the dominant transition and the free exciton (X_A and X_B) emission [15]. Particularly the D^0X linewidth of 870 μeV demonstrates the good crystal quality of these layers. To compare, it should be noted that FWHM values in the range below 1 meV have been reported from samples grown by HVPE [21] with comparably thick layers of several tens of μm but not from samples grown in MOVPE as in the present case. [19]. One disadvantage of the SiN interlayer was the background doping concentration determined by van-der-Pauw Hall measurements (n=$6 \cdot 10^{17}\,\mathrm{cm}^{-3}$; μ=$171\,\mathrm{cm}^2/\mathrm{Vs}$). Although no influence of the background doping on the optical properties was visible (Fig. 3) the SiN interlayer

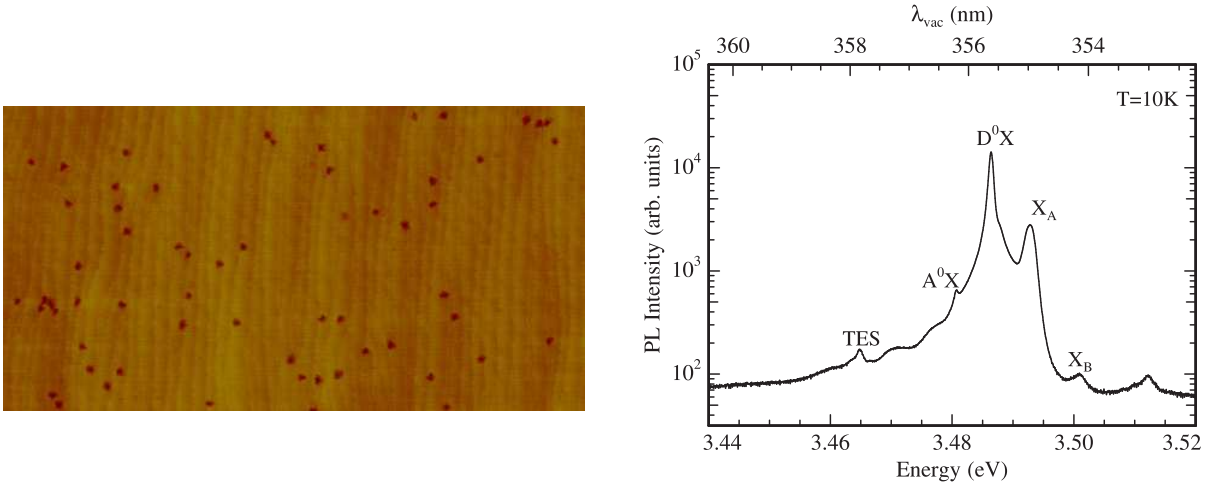

Fig. 3: Left: EPD of a nominally undoped GaN sample with SiN interlayer. The scan size was approximately $2.5\,\mu\mathrm{m} \times 5\,\mu\mathrm{m}$. Right: PL spectrum near the band gap measured at low temperature (10K). X_A and X_B refer to A- and B-valence band exciton, respectively. D^0X denotes donor bound exciton emission with its two-electron satellites (TES).

should not be implemented in HEMT structures, where a semi-insulating buffer is of great importance [22]. Only if the spacing between the SiN layer and the 2DEG would be large enough, carriers from the interlayer would not affect the device performance.

7. Device Performance

We already verified the good crystal quality of our GaN samples with the standard methods like DIC, AFM, HRXRD, PL and Hall. Additionally, we studied their influence on AlGaN/AlN/GaN high electron mobility transistor (HEMT) structures, which are well known as devices with high sensitivity in terms of crystal quality. The surface roughness as well as the dislocation density are only two figures of merit with crucial influence on the carrier mobility in the 2DEG. As we optimized both, we could realize HEMT structures (without SiN interlayer) with a low sheet resistance of $330\,\Omega/\square$ (295 K). In Hall measurement we determined the 2DEG carrier density to $1.1 \cdot 10^{13}\,\mathrm{cm}^{-2}$ and measured a mobility of $1720\,\mathrm{cm}^2/\mathrm{Vs}$. At low temperature (77 K), we determined a mobility of more than $10000\,\mathrm{cm}^2/\mathrm{Vs}$ with a carrier density of $1.3 \cdot 10^{13}\,\mathrm{cm}^{-2}$ ($50\,\Omega/\square$). Although these values are quite promising they don't reach the best values of Miyoshi et al. ($302\,\Omega/\square$) as they reported a dislocation density of about $3 \cdot 10^8\,\mathrm{cm}^{-2}$ in their HEMT samples [23]. If we include our SiN-Interlayer in the structure reducing the dislocation density to $4 \cdot 10^8\,\mathrm{cm}^{-2}$ we can determine a sheet resistance of about $310\,\Omega/\square$, what would be in nice agreement with Miyoshi et al. As our X-ray peaks are reported to be very narrow it was possible to get excellent omega-2-theta scans of our HEMT structure (Fig. 4). The thickness fringes of the 30 nm thick AlGaN ($\approx$ 30% Al) cap are noted at the low and high-angle side, respectively. Additionally one can see the AlN peak from the nucleation layer and the peak from the GaN-buffer. The large number of visible fringes confirm nicely our excellent crystal quality [24, 25] and the abruptness of our AlGaN/AlN/GaN-interfaces.

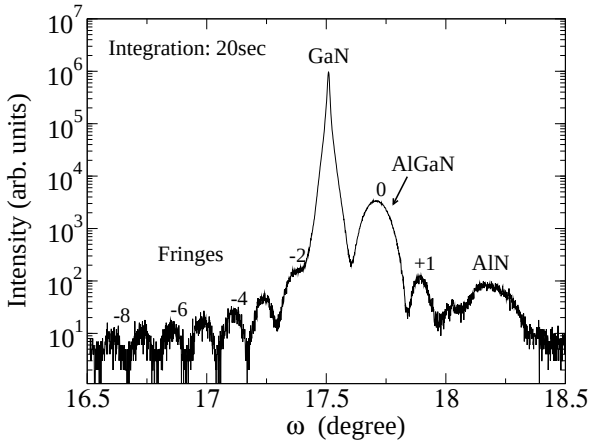

Fig. 4: X-ray diffraction profile of an AlGaN/AlN/GaN HEMT structure.

8. Summary

We demonstrated the optimization of the growth process for our nucleation layer and GaN-buffer. We found that oxygen doping during the nucleation process is of tremendous importance as well as prereactions between TMAl and ammonia were found to be critical. Additionally we demonstrated that the temperature ramp subsequent to the nucleation affects the surface roughness and the crystal quality of the GaN-buffer. We found that a very fast temperature ramp and short annealing time yields the best results. In terms of buffer layer optimization we concluded to grow with a reduced reactor pressure of 100 mbar, resulting in a highly efficient growth with further improved crystal quality. Finally we could reduce the dislocations in our samples by using an in-situ deposited SiN interlayer. With this low dislocation density we could achieve extremely good optical quality material, which was illustrated by a PL linewidth of the donor-bound exciton of 870 µeV (10K). As we used HEMT structures as a probe for our optimization steps, we could confirm excellent crystal properties.

9. Acknowledgment

This research was financially supported by Osram Opto Semiconductors and the Bundesministerium für Bildung und Forschung (BMBF). The sample characterization by M. Feneberg, E. Fuentes, C. Gao, and H. Xu is gratefully acknowledged.

References

[1] H. Amano, N. Sawaki, I. Akasaki, Y. Toyoda, *Appl. Phys. Lett.*, vol. 48, no. 5, pp. 353–355, 1986.

[2] S. Nakamura, *Jpn. J. Appl. Phys.*, vol. 30, no. 10A, pp. L1705-L1707, 1991.

[3] S.D. Lester, F.A. Ponce, M.G. Crawford, D.A. Steigerwald, *Appl. Phys. Lett.*, vol. 66, no. 10, pp. 1249–1251, 1995.

[4] T. Sugahara, H. Sato, M. Hao, Y. Naoi, S. Kurai, S. Tottori, K. Yamashita, K. Nishino, L.T. Romano, S. Sakai, *Jpn. J. Appl. Phys.*, vol. 37, no. 4A, pp. L398–L400, 1998.

[5] C.S. Tomiya, H. Nakajima, K. Funato, T. Miyjima, K. Kobaijashi, T. Hino, S. Kijima, T. Assano, M. Ikeda, *phys. stat. sol. (a)*, vol. 188, no. 1, pp. 69–72, 2001.

[6] D. Zanato, S. Gokden, N. Balkan, B.K. Ridley, W.J. Schaff, *Semicond. Sci. Technol.*, vol. 19, pp. 427–432, 2004.

[7] M. Miyoshi, T. Egawa, H. Ishikawa, K.-I. Asai, T. Shibata, M. Tanaka, O. Oda, *J. Appl. Phys.*, vol. 98, pp. 063713-1–063713-5, 2005.

[8] S. Tanaka, M. Takeuchi, Y. Aoyagi, *Jpn. J. Appl. Phys.*, vol. 39, no. 8B, pp. L831–L834, 2000.

[9] K.J. Lee, E.H. Shin, K.Y. Lim, *Appl. Phys. Lett.*, vol. 85, no. 9, pp. 1502–1504, 2004.

[10] K. Engl, M. Beer, N. Gmeinwieser, U.T. Schwarz, J. Zweck, W. Wegscheider, . Miller, A. Miler, H.-J. Lugauer, G. Brüderl, A. Lell, V. Härle, *J. Crystal Growth*, vol. 289, pp. 6–13, 2006.

[11] O. Contreras, F.A. Ponce, J. Christen, A. Dadgar, A. Krost, *Appl. Phys. Lett.*, vol. 81, no. 25, pp. 4712–4714, 2002.

[12] B. Kuhn, F. Scholz, *phys. stat. sol. (a)*, vol. 188, no. 2, pp. 629–633, 2001.

[13] J. Hertkorn et al., to be published in *J. Crystal Growth*, 2007.

[14] J.-H. Kim, S.C. Choi, K.S. Kim, G.M. Yang, C.-H. Hong, K.Y. Lim, H.J. Lee, *Jpn. J. Appl. Phys.*, vol. 38, no. 5A, pp. 2721–2724, 1999.

[15] K. Kornitzer, T. Ebner, M. Grehl, K. Thonke, R. Sauer, C. Kirchner, V. Schwegler, M. Kamp, M. Leszczynski, I. Grzegory, S. Porowski, *phys. stat. sol. (b)*, vol. 216, pp. 5–9, 1999.

[16] T. Hino, S. Tomiya, T. Miyajima, K. Yanashima, S. Hashimoto, M. Ikeda, *Appl. Phys. Lett.*, vol. 76, no. 23, pp. 3421–3423, 2000.

[17] T. Miyajima, T. Hino, S. Tomiya, K. Yanashima, H. Nakajima, T. Araki, Y. Nanishi, A. Satake, Y. Masumoto, K. Akimoto, T. Kobayashi, M. Ikeda, *phys. stat. sol. (b)*, vol. 228, no. 2, pp. 395–402, 2001.

[18] F. Habel, M. Seyboth, *phys. stat. sol. (c)*, vol. 0, no. 7, pp. 2448–2451, 2001.

[19] B. Heying, X.H. Wu, S. Keller, Y. Li, D. Kapolnek, B.P. Keller, S.P. DenBaars, J.S. Speck, *Appl. Phys. Lett.*, vol. 68, no. 23, pp. 643–645, 1996.

[20] L. Sugiura, K. Itaya, J. Nishio, H. Fujimoto, Y. Kokubun, *J. Appl. Phys.*, vol. 82, pp. 4877–4882, 1997.

[21] P. Brückner et al., to be published in *J. Crystal Growth*, 2007.

[22] Z. Bougrioua, M. Azize, A. Jimenez, A-F. Braña, P. Lorenzini, B. Beaumont, E. Muñoz, P. Gibart, it phys. stat. sol. (c), vol. 2, no. 7, pp. 2424–2428, 2005.

[23] M. Miyoshi, A. Imanishi, T. Egawa, H. Ishikawa, K.-I. Asai, T. Shibata, M. Tanaka, O. Oda, *Jpn. J. Appl. Phys.*, vol. 44, no. 9A, pp. 6490–6494, 2005.

[24] A. Torabi, P. Ericson, E.J. Yarranton, W.E. Hoke, *J. Vac. Sci. Technol. B*, vol. 20, pp. 1234–1237, 2002.

[25] N. Tang, B. Shen, M.J. Wang, Z.J. Yang, K. Xu, G.Y. Zhang, T. Lin, B. Zhu, W.Z. Zhou, J.H. Chu, *Appl. Phys. Lett.*, vol. 88, pp. 172115-1–172115-3, 2006.